Available online at www.sciencedirect.com

SCIENCE DIRECT®

Bioorganic & Medicinal Chemistry 13 (2005) 1977–1988

Bioorganic & Medicinal Chemistry

Conformational restrictions in ligand binding to the human intestinal di-/tripeptide transporter: implications for design of hPEPT1 targeted prodrugs

Jon Våbenø,[a] Carsten Uhd Nielsen,[b] Bente Steffansen,[b] Tore Lejon,[c] Ingebrigt Sylte,[d] Flemming Steen Jørgensen[e] and Kristina Luthman[a,f,*]

[a]*Department of Medicinal Chemistry, Institute of Pharmacy, University of Tromsø, N-9037 Tromsø, Norway*
[b]*Molecular Biopharmaceutics, Department of Pharmaceutics, The Danish University of Pharmaceutical Sciences, Universitetsparken 2, DK-2100 Copenhagen, Denmark*
[c]*Department of Chemistry, University of Tromsø, N-9037 Tromsø, Norway*
[d]*Department of Pharmacology, Institute of Medical Biology, University of Tromsø, N-9037 Tromsø, Norway*
[e]*Department of Medicinal Chemistry, The Danish University of Pharmaceutical Sciences, Universitetsparken 2, DK-2100 Copenhagen, Denmark*
[f]*Department of Chemistry, Medicinal Chemistry, Göteborg University, SE-412 96 Göteborg, Sweden*

Received 14 September 2004; revised 5 January 2005; accepted 12 January 2005

Abstract—The aim of the present study was to develop a computational method aiding the design of dipeptidomimetic pro-moieties targeting the human intestinal di-/tripeptide transporter hPEPT1. First, the conformation in which substrates bind to hPEPT1 (the bioactive conformation) was identified by conformational analysis and 2D dihedral driving analysis of 15 hPEPT1 substrates, which suggested that $\psi_1 \sim 165°$, $\omega_1 \sim 180°$, and $\varphi_2 \sim 280°$ were descriptive of the bioactive conformation. Subsequently, the conformational energy required to change the peptide backbone conformation (ΔE_{bbone}) from the global energy minimum conformation to the identified bioactive conformation was calculated for 20 hPEPT1 targeted model prodrugs with known K_i values. Quantitatively, an inverse linear relationship ($r^2 = 0.81$, $q^2 = 0.80$) was obtained between ΔE_{bbone} and log $1/K_i$, showing that ΔE_{bbone} contributes significantly to the experimentally observed affinity for hPEPT1 ligands. Qualitatively, the results revealed that compounds classified as high affinity ligands ($K_i < 0.5$ mM) all have a calculated $\Delta E_{\text{bbone}} < 1$ kcal/mol, whereas medium and low-affinity compounds ($0.5 \text{ mM} < K_i < 15$ mM) have ΔE_{bbone} values in the range 1–3 kcal/mol. The findings also shed new light on the basis for the experimentally observed stereoselectivity of hPEPT1.

---

1. Introduction

One decade after the cloning of the first mammalian intestinal di-/tripeptide transporter,[1] the human ortholog hPEPT1,[2] is still receiving considerable attention.[3–8] This is attributed to its ability to transport not only peptides but also peptidomimetic drugs (e.g., β-lactam antibiotics[9] and ACE inhibitors[10]) and prodrugs based on single amino acids or dipeptidic pro-moieties.[11,12] hPEPT1 recognizes peptides ranging in size from Gly-Gly to Trp-Trp-Trp (K_i values of 1.0 and 0.15 mM, respectively[8]) and is known as a promiscuous transporter. For these reasons, prodrug targeting to hPEPT1 provides an intriguing alternative strategy for improving drug transport across biological barriers expressing hPEPT1, that is, the intestinal wall. The best example to date of a prodrug actively transported by hPEPT1 is the marketed compound valacyclovir (the L-valyl ester of acyclovir),[13,14] thus, a drug/prodrug delivery approach targeting hPEPT1 holds great promise. The fact that natural dipeptides are not suited as pro-moieties due to their enzymatic instability in the gastrointestinal tract has initiated an extensive search for other potential pro-moieties. The main focus of our research is to examine the possibility of using dipeptidomimetic compounds for this purpose.

Keywords: Bioactive conformation; Conformational energy; Intestinal di-/tripeptide transporter; PEPT1.

* Corresponding author. Tel.: +46 31 772 2894; fax: +46 31 772 3840; e-mail: luthman@chem.gu.se

0968-0896/$ - see front matter © 2005 Elsevier Ltd. All rights reserved.
doi:10.1016/j.bmc.2005.01.019

The 3D structure of hPEPT1 has not yet been determined, however, indirect evidence for the transporter topology has been obtained based on epitope tagging[15] and site directed mutagenesis studies.[16–21] The lack of detailed structural information suggests that protein modeling combined with docking studies currently is of limited value, and ligand-based design is therefore crucial in order to extract further structure–affinity relationships. To investigate the possible use of pro-moieties with different structural modifications (i.e., inverted side chain stereochemistry or amide bond replacement), binding affinity, and transport via hPEPT1 have been investigated for a number of prodrugs and model prodrugs.[22–27] However, synthesis and biological investigations are quite labor demanding, and a computational screening procedure for prediction of hPEPT1 affinity for pro-moieties/prodrugs would therefore be a considerable advantage.[28]

The significance of L,L-stereochemistry[29] and *trans*-orientation of the peptide bond[30,31] for optimal hPEPT1 affinity of dipeptides has been known for some time. Less is known about conformational effects and backbone flexibility. These aspects are of considerable importance as the conformational energy penalty that the ligand has to pay in order to adopt the binding conformation is a critical factor for the affinity. Therefore, identification of the conformation in which ligands bind to hPEPT1 (hereafter called the bioactive conformation) is vital in order to enable a successful design of pro-moieties. Bailey et al. proposed the first general 3D substrate template for hPEPT1,[32] however, this template was partly based on biological data from affinity studies performed using renal brush-border membrane vesicles from rat,[33] expressing both PEPT1 and the renal isoform PEPT2. K_i values for PEPT2 are generally 10- to 100-fold lower than for PEPT1,[7,34] indicating that the structure–affinity relationships obtained could be misleading.[35] Recently a more detailed pharmacophore model for hPEPT1 was proposed by Gebauer et al.[36] describing the optimal steric, electrostatic, hydrophobic, hydrophilic, and H-bond properties based on CoMFA/CoMSIA studies. However, the bioactive conformation in that study was identified based on a common energy minimum for only two compounds (Ala-Ala and AlaΨ[CS–N]Pro). Moreover, several of the reported conformational energy penalties seemed unreasonable, for example, a value of 0.0 kcal/mol for all four stereoisomers of Ala-Ala. These values are unlikely to account for the stereoselectivity observed for ligand binding to hPEPT1, which has a preference for compounds with all L-configuration[29,37,38] even if appreciable affinities have been reported for both dipeptides and dipeptide derivatives with L,D-, D,L-, and D,D-configurations.[39]

In order to provide insight into the relationship between conformational preference and affinity for hPEPT1 ligands, we have in the present study set out to calculate conformational energy penalties for a series of 20 hPEPT1 targeted model prodrugs with pro-moieties based on different stabilizing principles. Calculation of the energetic penalty requires knowledge of (1) the bioactive conformation, and (2) the preferred conformation of the molecule. Here we present molecular modeling studies performed in a simulated protein environment for a series of diverse hPEPT1 substrates, whereby a reliable estimate of the bioactive conformation for binding to hPEPT1 could be obtained. Subsequent calculations of the conformational energy required for *the peptide backbone* to adopt this conformation enabled a rationalization of the affinities of the 20 model prodrugs.

2. Results and discussion

2.1. Identification of the bioactive conformation for binding to hPEPT1

The approach taken for identifying the bioactive conformation for hPEPT1 binding was to examine the conformational preferences of a series of β-lactam antibiotics known as hPEPT1 substrates with experimentally determined K_i values. This class of compounds was selected based on their tripeptidomimetic nature and the structural rigidity resulting from the bicyclic β-lactam moiety. As a result of the reduced flexibility, a limited number of energetically allowed conformations was expected, simplifying the interpretation of the 2D dihedral driving analysis. The results from these initial investigations could then be validated and refined by similar calculations using dipeptidic and dipeptidomimetic hPEPT1 substrates. The MMFFs force field[40] was used for the energy calculations, since MMFF has been shown to be the best force field (along with the MM2/MM3-based force fields) for reproducing experimental conformational energies.[41]

2.1.1. β-Lactam antibiotics

2.1.1.1. Compound selection. A series of nine structurally similar α-amino substituted β-lactam antibiotics (**1**–**9**; five cephalosporins, two carbacephems, and two penicillins) were selected from the literature (Fig. 1, Table 1). A misguiding interpretation of the names L-cephalexin and L-loracarbef from the literature needed to be corrected. These two compounds were originally presented as enantiomers of cephalexin and loracarbef, respectively,[37] but are really diastereomers (α-epimers) as classified in CAS. The correct structures are shown in Figure 1. Care must be taken when giving quantitative interpretations of K_i values for β-lactam antibiotics from the literature since different values have been reported for the same compound, most often due to different experimental conditions. The K_i values for compounds **1**–**8** were obtained under similar experimental conditions,[9,42,43] whereas the K_i value for L-loracarbef (**9**) was from a study by Wenzel et al.[37] where pH 6.5 was used in the apical compartment instead of the commonly used pH 6.0 (used for **1**–**8**). For these zwitterionic compounds differences in pH may result in a shift between different protonation states, which in turn can result in a change in the observed affinity. Wenzel et al.[37] obtained a K_i value of 0.5 mM at pH 6.5 for L-cephalexin (**7**), which is comparable to the value (0.8 mM) reported by Dantzig and Bergin at pH 6.0.[42] This indicates that the affinity of **9** (K_i 0.7 mM) should be similar to that of **7**. Thus, in the context of the present study,

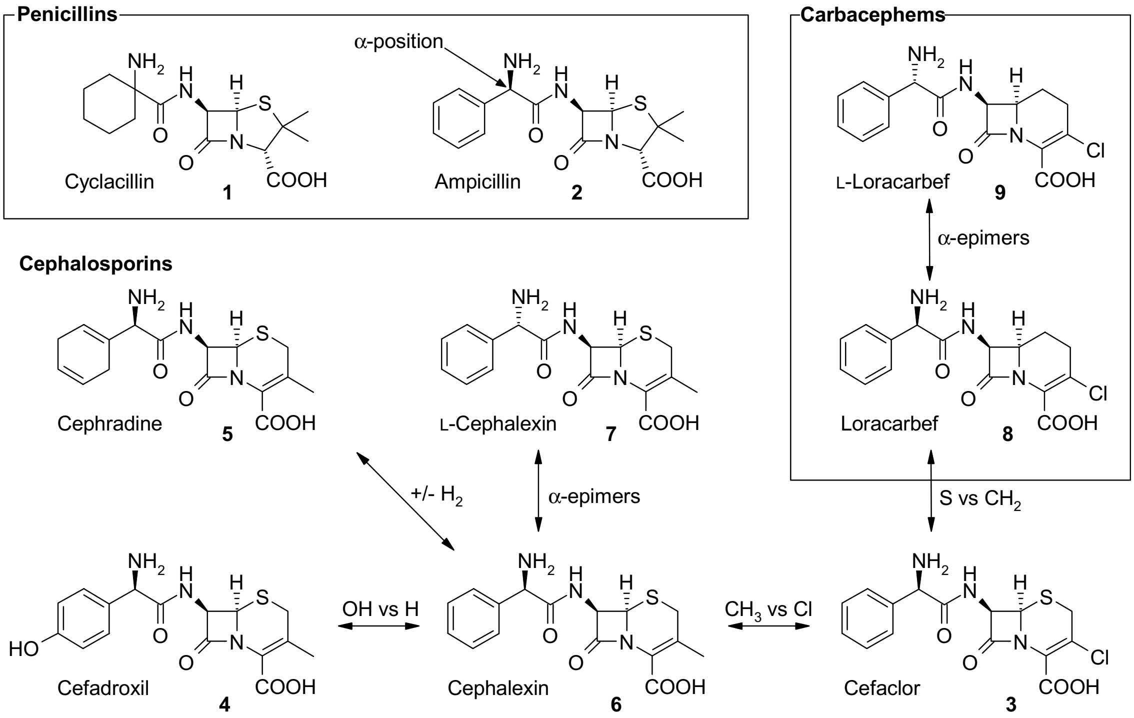

Figure 1. Structures of the nine α-amino β-lactam antibiotics **1**–**9** used to identify plausible bioactive conformations, including their structural relationships.

Table 1. α-Configuration, selected torsion angles (ψ_1, ω_1, and φ_2)[a] for the calculated global energy minimum conformations in vacuo, experimental K_i values and affinity classification for the nine α-amino β-lactam antibiotics **1**–**9**

No.	Compound	α-config.	ψ_1	ω_1	φ_2	K_i (mM)	Affinity classification	Ref.
1	Cyclacillin	Symmetrical	180	182	180	0.5	High	9
2	Ampicillin	D	202	183	181	14.5	Low	9
3	Cefaclor	D	203	182	190	11	Low	9
4	Cefadroxil	D	203	183	190	7.2	Low	9
5	Cephradine	D	208	184	190	9.8	Low	9
6	Cephalexin	D	203	183	190	9.2	Low	42
7	L-Cephalexin	L	166	176	284	0.8	High	42
8	Loracarbef	D	203	183	178	11.6	Low	43
9	L-Loracarbef	L	156	180	176	0.7	High	37

[a] For definitions of the ψ_1, ω_1, and φ_2 angles, see Figure 2.

compounds **1**, **7**, and **9** were regarded as high affinity compounds, and the remaining six as low-affinity compounds (Table 1).

2.1.1.2. Conformational analysis and 2D dihedral driving analysis in vacuo.

The compounds were first submitted to conformational analysis in vacuo in order to obtain the global energy minimum conformation. The results showed that the β-lactam derivatives preferred a conformation with a torsion angle $\varphi_2 \sim 180°$ (for torsion angle definitions, see Fig. 2), except for L-cephalexin (**7**), which preferred an angle of 284° (Table 1). The ψ_1 angles varied in a more continuous manner between 156° and 208°, the ψ_1 angles of the high affinity compounds **1**, **7**, and **9** being in the lower part of the interval.

The first indications of the effect of the amide bond conformation on PEPT1/PEPT2 affinity came from a study

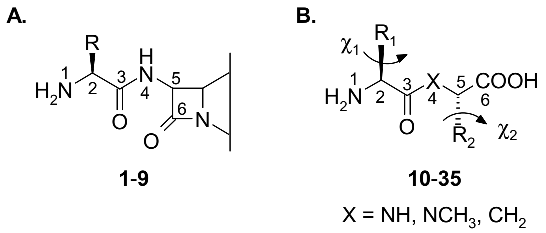

Figure 2. Definitions of the torsion angles ψ_1 (1–2–3–4), ω_1 (2–3–4–5), and φ_2 (3–4–5–6) for **1**–**9** (A) and **10**–**35** (B). Structure B also shows the general structure of a stabilized pro-moiety for hPEPT1-mediated transport (**16**–**35**). When X = NH, one of the stereocenters (atom 2 or atom 5) is D-configured. R_{attach} is the side chain functioning as model drug attachment point (Asp, Glu, Orn, Lys), and R_{bbone} is the side chain not involved in the attachment (Gly, Ala, Val, Phe). When $R_1 = R_{attach}$ then $R_2 = R_{bbone}$, and vice versa. For compounds with a non-symmetric R_{bbone} (Val, Phe) three different conformations could be obtained due to the rotational barriers of the χ torsion for R_{bbone}.

on renal brush-border membrane vesicles.[33] Studies on Caco-2 cells have later confirmed that a *trans*-orientation of the *N*-terminal amide bond ($\omega_1 \sim 180°$) is crucial for hPEPT1 affinity,[30,31] indicating that the main conformational freedom for hPEPT1 substrates containing an amide bond, such as β-lactams, is limited to the ψ_1 and φ_2 torsions of the β-lactam side chain. Thus, in order to obtain an overview of the energy contour surface, the global energy minimum conformation of each compound was submitted to a 2D dihedral driving analysis in vacuo. The 2D plots of the relative energy versus ψ_1 and φ_2 revealed that the nine β-lactam derivatives **1**–**9** all had energy minima (global or local) at both $\varphi_2 \sim 180°$ and ~280° (Fig. 3). The shape of the energy contour map for cephalexin (**6**) was qualitatively similar to those for compounds **2**–**5** (Table 1). The trend observed for ψ_1 was also evident, as the minima were shifted toward 160° for the high affinity L-configured compounds (**7** and **9**), and toward 180° for the high affinity α-symmetric compound cyclacillin (**1**). In contrast, the ψ_1 angles of the six low-affinity D-configured compounds **2**–**6** and **8** all were in the interval 200–210°. Thus, for the nine β-lactams two conformations representing a plausible bioactive backbone conformation for binding to hPEPT1 were identified, described by (A) $\psi_1 \sim 165°$, $\omega_1 \sim 180°$, $\varphi_2 \sim 280°$, and (B) $\psi_1 \sim 165°$, $\omega_1 \sim 180°$, $\varphi_2 \sim 180°$ (Fig. 4).

β-Lactam antibiotics represent a class of compounds that has been the focus of similar studies earlier, and conflicting theories have been proposed. Bailey et al.[32] described a φ_2 angle of ~300° for the bioactive conformation of peptides and peptidomimetics. However, a deviation from the template backbone was proposed for β-lactams, where the carbon–nitrogen bond protruding from the lactam moiety was rotated 180°, corresponding to a φ_2 of approximately 120°. In the present study the 2D dihedral driving analysis revealed that a φ_2 angle in the interval 80–120° at best represents a saddle point on the energy contour surface, with very high

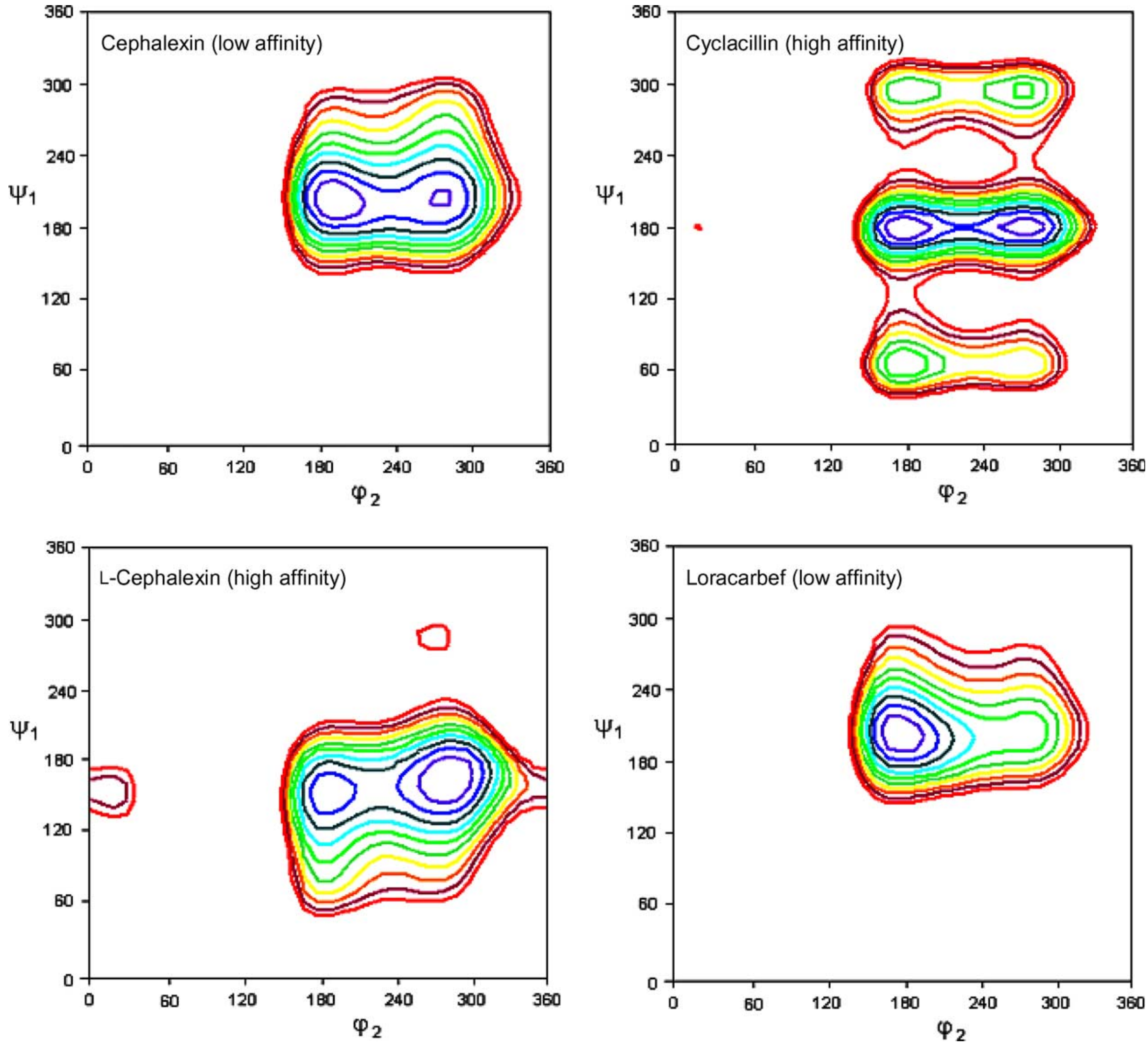

Figure 3. Energy contour maps for cephalexin (**6**), cyclacillin (**1**), L-cephalexin (**7**), and loracarbef (**8**) in vacuo. For clarity only the parts of the map corresponding to $\Delta E < 3.6$ kcal/mol (15 kJ/mol) are shown. The energy isocontours represent energy increments of 0.3 kcal/mol.

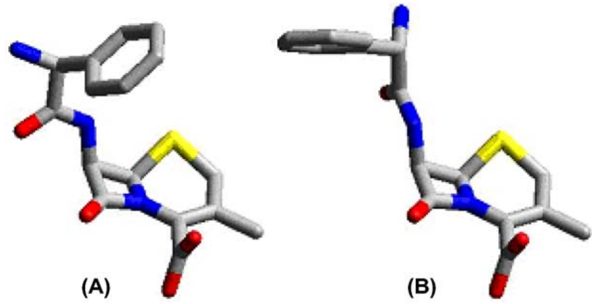

Figure 4. The two low energy conformations for L-cephalexin (**7**): (A) $\varphi_2 \sim 280°$ (global minimum); (B) $\varphi_2 \sim 180°$ ($\Delta E = 0.4$ kcal/mol). Hydrogen atoms are omitted for clarity.

energy (ΔE typically 10–14 kcal/mol for **1**–**9**, results not shown). In a molecular modeling study of the structural requirements for binding to the renal di-/tripeptide transporter PEPT2 a φ_2 of approximately 180° was proposed for cephalosporins, whereas two possible ψ_1 torsions (~50° and ~210°) were suggested.[44] Swaan and Tukker proposed a pharmacophore map for PEPT1 based on penicillins, cephalosporins, and ACE inhibitors in which the torsions of the backbone were not explicitly described.[45] However, visual inspection of the pharmacophore in a CoMFA-study subsequently published by the same group[46] revealed that a φ_2 of approximately 180° had been used in the alignment of the β-lactams, that is, a conformation similar to that shown in Figure 4B.

2.1.2. Dipeptides and dipeptidomimetics

2.1.2.1. Compound selection. In order to determine which of the two possible conformations (A or B) that was most likely the bioactive one, the investigations were extended to include dipeptides and dipeptidomimetics also. Thus, three dipeptides (**10**–**12**; Gly-Gly, Ala-Ala, and Phe-Ala), two dipeptidic ketomethylene isosteres (**13**–**14**; δ-aminolevulinic acid (δ-ALA), and PheΨ[$COCH_2$]Gly) and one *N*-methylated dipeptide (**15**; Gly-Sar = GlyΨ[$CON(CH_3)$]Gly) (Fig. 5) were included in the series of compounds. The dipeptides represent natural hPEPT1 substrates, while **13** (a Gly-Gly mimetic) and **14** (a Phe-Gly mimetic) both display hPEPT1 affinity and transport.[47–50] Compound **15** is a widely used reference compound for studies of hPEPT1 affinity and transport. This compound was included due to its conformational restrictions (compared to natural dipeptides) resulting from the *N*-methylation, an observation that has been addressed earlier.[51] These six compounds all possess the structural features considered important for optimal hPEPT1 binding (free *N*- and *C*-termini, a carbonyl group, and correct stereochemistry where applicable). As compounds **13** and **15** are Gly-Gly analogues, the main determinant for their affinities is expected to reside in their ability to adopt the bioactive conformation.

2.1.2.2. Conformational analysis and 2D dihedral driving analysis in vacuo. The conformational search in vacuo resulted in an all-*trans* conformation for the achiral Gly-Gly (**10**), whereas the two substituted dipeptides **11** and **12** preferred virtually identical conformations, with the backbone slightly tilted (Table 2). The ketomethylene isosteres **13** and **14** both preferred a cyclic conformation, corresponding to the global energy minimum in vacuo. This conformation was stabilized by strong electrostatic and H-bond interactions between the oppositely charged *N*- and *C*-termini, resulting in an eight-membered cyclic structure. This can be explained by the increased flexibility of the ketomethylene isosteres compared to the natural dipeptides in which the preference for a *trans*-orientation of the amide bond prevents the cyclic conformation. The effect has been termed 'electrostatic collapse'[52] and is a result of insufficient shielding of the charges in the computational method used. A similar preference for a cyclic conformation was observed also for **15**, which preferentially adopted a *cis*-amide bond arrangement in its global energy minimum conformation in vacuo. It is generally accepted that *N*-methylation of an amide bond results in an increased population of the *cis*-conformation due to steric

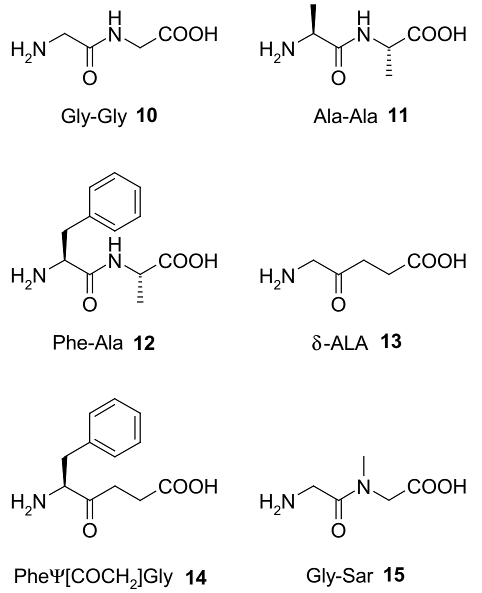

Figure 5. Structures of the six dipeptides and dipeptidomimetics **10**–**15** used for the refinement of the bioactive conformation.

Table 2. Selected torsion angles (ψ_1, ω_1, and φ_2)[a] for the calculated global energy minimum conformations in vacuo and experimental K_i values for the six dipeptides and dipeptidomimetics **10**–**15**

No.	Compound	ψ_1	ω_1	φ_2	K_i (mM)	Ref.
10	Gly-Gly	180	180	180	0.86	63
11	Ala-Ala	165	180	201	0.08	31
12	Phe-Ala	162	180	201	0.18	49
13	δ-ALA[b]	97	239	71	2.2	63
14	PheΨ[$COCH_2$]Gly[b]	118	265	73	0.4	49
15	Gly-Sar[c]	87[d]	357[d]	266[d]	0.83	31
		188[e]	172[e]	261[e]		

[a] For definitions of the ψ_1, ω_1, and φ_2 angles, see Figure 2.

[b] Cyclic conformation.

[c] The calculated energy difference between the lowest energy conformations with *cis*- and *trans*-orientation of the amide bond was 2.8 kcal/mol.

[d] *cis*-Conformation.

[e] *trans*-Conformation.

effects, which also brings the *N*- and *C*-terminal charges in close proximity. Thus, the calculated energy of the resulting conformation in vacuo can be expected to be (artificially) lower than for the *trans*-conformation with lowest energy.

For compounds **13–15** the 'electrostatic collapse' was counteracted by applying a torsional constraint on ω_1 of 180 ± 5° in the 2D analyses, such that the energy contour surface only for conformations corresponding to a *trans*-amide geometry was described. The 2D energy contour maps for compounds **10**, **11**, **13**, and **15** are shown in Figure 6. The contour maps for Ala-Ala (**11**) and δ-ALA (**13**) are qualitatively similar to the maps for Phe-Ala (**12**) and PheΨ[COCH$_2$]Gly (**14**), respectively (data not shown). However, for **14** the energy minima were shifted toward a ψ_1 angle of ~165°. Figure 6 reveals that the natural dipeptides **10–12** have conformational preferences similar to the β-lactams, with a global energy minimum corresponding to $\varphi_2 \sim 180°$ and a local minimum at $\varphi_2 \sim 280°$. In contrast, the ketomethylene isosteres **13–14** prefer a conformation with a φ_2 angle of 280°. This is even more pronounced for the *N*-methylated dipeptide Gly-Sar (**15**), where $\varphi_2 = 180°$ represents a saddle point, with relatively high energy. The latter finding strongly suggests that $\varphi_2 \sim 180°$ is not a plausible torsion for the bioactive conformation for hPEPT1 binding. As for the β-lactams, ψ_1 for the achiral compounds (Gly-Gly and its analogues **13** and **15**) was approximately 180°, while the compounds with L-configuration (**11**, **12**, and **14**) showed a preference for ψ_1 of approximately 165°.

In summary, the combined trends in the conformational propensities of the β-lactam antibiotics **1–9** and the dipeptides/-mimetics **10–15** strongly suggest that

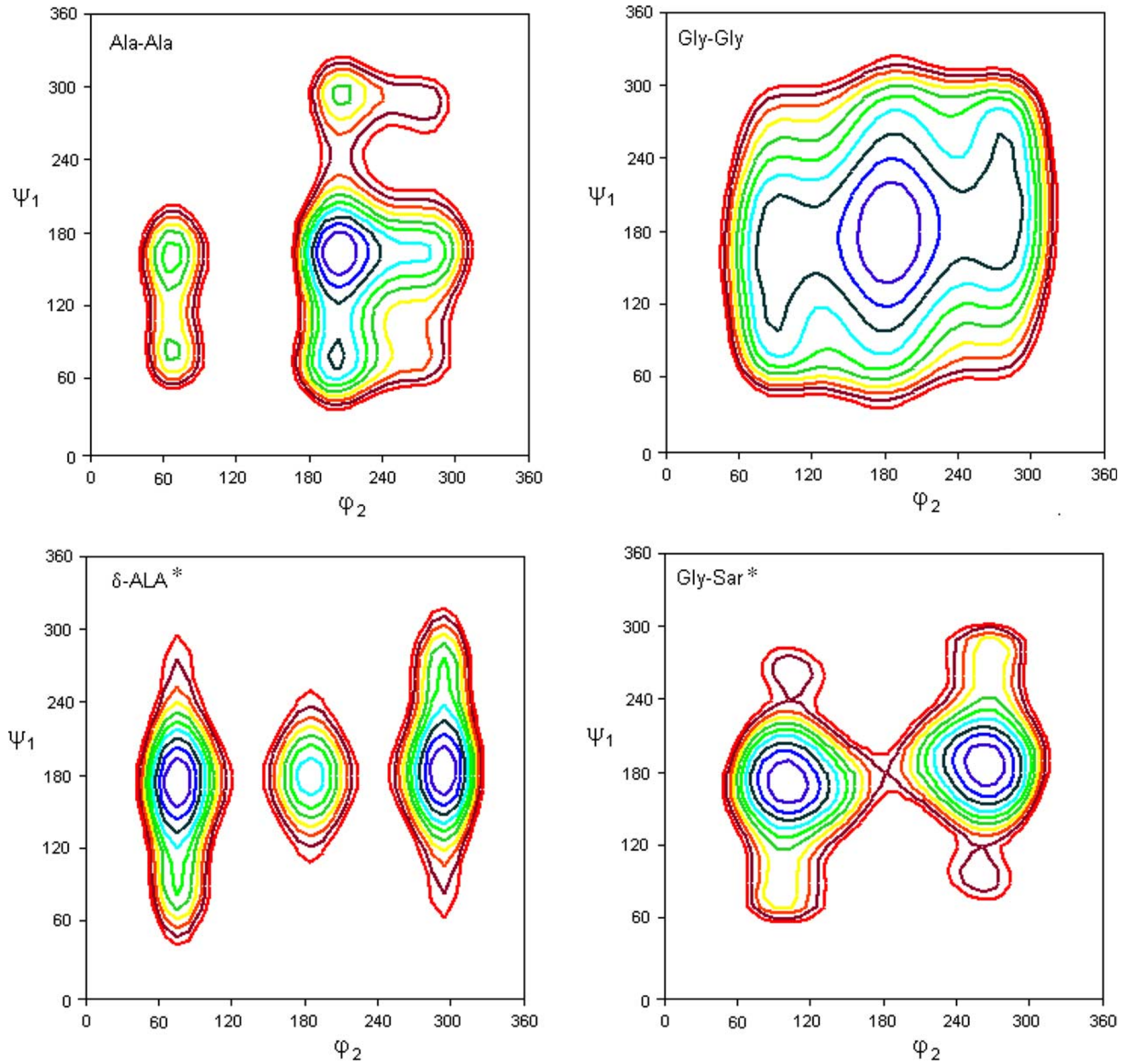

Figure 6. Energy contour maps for Ala-Ala (**11**), Gly-Gly (**10**), δ-ALA (**13**), and Gly-Sar (**15**) in vacuo. For clarity only the parts of the map corresponding to $\Delta E < 3.6$ kcal/mol (15 kJ/mol) are shown. The energy isocontours represent energy increments of 0.3 kcal/mol. *ω_1 constrained to 180 ± 5° during the 2D dihedral driving.

$\psi_1 \sim 165°$, $\omega_1 \sim 180°$, and $\varphi_2 \sim 280°$ are descriptive of the bioactive backbone conformation for optimal binding to hPEPT1. Deviations from the optimal torsion angles must be expected at the binding site due to the dynamic nature of the ligand–target complexation. However, such deviations are restricted, and for simplicity the exact values were used in the subsequent calculations. It should be mentioned that despite the methodological weakness of the study by Gebauer et al.[36] the reported bioactive conformation ($\psi_1 = 142$–$165°$, $\omega_1 \sim 180°$, and $\varphi_2 = 262$–$302°$) turns out to be in good agreement with the results of the present study.

2.2. Conformational properties of model prodrugs targeting hPEPT1

The overall goal of the present study was to develop a modeling tool useful for designing dipeptidic pro-moieties in a prodrug approach targeting hPEPT1. When introducing a drug with unfavorable intrinsic biopharmaceutical properties in a prodrug structure for hPEPT1, the affinity is likely to decrease. Thus, the hPEPT1 affinity of the pro-moiety must be optimized to compensate for these negative effects, such that a maximum degree of recognition is retained. This means that seemingly marginal contributions of pro-moiety optimization could turn out to be crucial for the success (or failure) of a prodrug approach targeting hPEPT1.

Even if derivatization of the *N*- or *C*-termini does not abolish affinity, free end groups have proven to be important pharmacophore elements.[53] Thus, we consider the R_1- or R_2-positions (Fig. 2B) as the two relevant drug attachment points for an optimal prodrug based on a dipeptidic pro-moiety. In order to introduce linkage diversity in the R_1 or R_2 position Asp or Glu side chains are the best alternatives, as the drug can then be attached via an ester or an amide bond (drug–OH, drug–NH_2). For drug–COOH, Ser, Thr, Tyr, and Lys side chain are obvious alternatives. As a correct *N*- to *C*-terminal distance in terms of spacer length has also proven to be important for PEPT1 affinity (β-amino acids are compatible, but unfavorable[54]) three different approaches have mainly been used in order to increase the enzymatic stability of the dipeptidic pro-moiety; incorporation of a D-amino acid, *N*-methylation of the amide bond, or the use of amide bond replacements such as the ketomethylene isostere (Fig. 2B).

The conformational energy required to adopt the bioactive conformation, $\Delta G_{\mathrm{conf(ligand)}}$, was chosen as the descriptor for the conformational properties of the compounds investigated in the present study. Different estimates for the upper limit of $\Delta G_{\mathrm{conf(ligand)}}$ have been suggested for pharmacophore identification.[55–57] In a rather comprehensive study by Nicklaus et al.[58] an average $\Delta G_{\mathrm{conf(ligand)}}$ of 15.9 kcal/mol was reported for protein binding of a diverse series of flexible ligands. However, in a similar study by Boström et al.[52] an upper limit of ~3 kcal/mol was indicated. The main reason for this large discrepancy seems to be that the results obtained by Nicklaus et al. were based on computational investigations in vacuo, in which intramolecular interactions are likely to be overestimated. This gives rise to larger conformational penalties upon reorganization of the global minimum conformation. In contrast, Boström et al. performed the calculations in a simulated water environment, which is computationally more demanding but is expected to reflect the real situation to a larger extent. Hence, the latter was the method of choice for calculation of $\Delta G_{\mathrm{conf(ligand)}}$ in the present study.

As the exact orientations of the side chains in the binding site of hPEPT1 are not known, it was decided to only study the energetic contribution from the peptide/peptidomimetic backbone, hereafter called $\Delta E_{\mathrm{bbone}}$ (for the definition of backbone, see Section 4). Thereby, the energy contribution resulting from the random positioning of the flexible R_{attach} side chain was removed.

2.2.1. Compound selection. The investigations were exclusively focused on pro-moieties representing the three different stabilizing principles mentioned above. As the objective was to consider only the contribution from the backbone ($\Delta E_{\mathrm{bbone}}$) to the overall $\Delta G_{\mathrm{conf(ligand)}}$ (and hence, to K_i) only compounds with relatively similar 'drugs' attached were included, such that the possible influence of the 'drug' on the experimental K_i values was reduced. Biological data for compounds conforming to this criterion is at present only available for model prodrugs. A further inclusion criterion was that reliable affinity data for hPEPT1 (i.e., K_i or IC_{50} values) was available. As K_i values above 15 mM are considered uninteresting,[8] only compounds with $K_i < 15$ mM were included. In total 20 dipeptide derivatives (**16**–**35**, Tables 3 and 4) were included into the data set, including five compounds based on natural dipeptides (Asp(OBn)-Ala, Lys(Z)-Ala, Ala-Lys(Z), Ala-Orn(Z), and Ala-Asp(OBn)) for comparison purposes. The model drug was either MeOH attached via an ester bond or BnOH attached via an ester or a carbamate linker. The pro-moieties utilizing R_1 as attachment point (**16**–**24**) were based on Asp-Ala, Glu-Ala, Lys-Ala, Glu-Val, Asp-Gly, and Glu-Gly motifs (Table 3), whereas the R_2

Table 3. Calculated $\Delta E_{\mathrm{bbone}}$ and experimental K_i values for the model prodrugs **16**–**24** with the R_1 side chain as drug attachment point

No.	Compound	$\Delta E_{\mathrm{bbone}}$[a] (kcal/mol)	K_i (mM)	Ref.
16	Asp(OBn)-Ala	0.46	0.10	27
17	D-Asp(OBn)-Ala	1.22	2.62[c]	64
18	D-Glu(OBn)-Ala[b]	1.84	5.47[c]	23
19	Lys(Z)-Ala	−0.08	0.11	39
20	D-Lys(Z)-Ala	1.85	9.30	39
21	Glu(OMe)-D-Val[b]	3.30	13.0	59
22	D-Glu(OMe)-Val[b]	1.52	1.85	59
23	Asp(OBn)-Sar[b]	−0.79	0.014[c]	64
24	Glu(OMe)-Sar[b]	0.21	0.36	59

[a] Energy of the aligned backbone relative to the backbone of the global energy minimum conformation in water after constrained relaxation.

[b] The conformation with lowest energy in water without evident intramolecular electrostatic/H-bond interactions between the *N*- and *C*-termini or intramolecular H-bond interactions between the backbone and the side chain was used as reference.

[c] The reported value is an IC_{50} value expected to be representative for the K_i value under the experimental conditions used.

Table 4. Calculated $\Delta E_{\mathrm{bbone}}$ and experimental K_i values for the model prodrugs **25**–**35** with the R_2 side chain as drug attachment point

No.	Compound	$\Delta E_{\mathrm{bbone}}$[a] (kcal/mol)	K_i (mM)	Ref.
25	Ala-Asp(OBn)	0.23	0.11	27
26	Ala-Lys(Z)[b]	0.04	0.18	39
27	Ala-D-Lys(Z)	1.78	2.50	39
28	D-Ala-Lys(Z)	2.51	2.30	39
29	Ala-Orn(Z)[b]	−0.03	0.52	39
30	Ala-D-Orn(Z)[b]	1.75	6.60	39
31	D-Ala-Orn(Z)[b]	2.48	1.90	39
32	Val-D-Glu(OMe)[b]	1.74	2.76	59
33	D-Val-Glu(OMe)[b]	3.11	11.0	59
34	PheΨ[$COCH_2$]Asp(OBn)	0.28	0.07	26
35	ValΨ[$COCH_2$]Asp(OBn)	−0.25	0.02	26

[a] Energy of the aligned backbone relative to the backbone of the global energy minimum conformation in water after constrained relaxation.

[b] The conformation with lowest energy in water without evident intramolecular electrostatic/H-bond interactions between the *N*- and *C*-termini or intramolecular H-bond interactions between the backbone and the side chain was used as reference.

attachments were based on Ala-Asp, Ala-Lys, Ala-Orn, Val-Glu, Phe-Asp, and Val-Asp motifs (**25**–**35**, Table 4). The structures of the ketomethylene-based prodrugs PheΨ[$COCH_2$]Asp(OBn) (**34**) and ValΨ[$COCH_2$]Asp-(OBn) (**35**) are shown in Figure 7. The methyl ester derivatives **21**, **22**, **24**, **32**, and **33** (previously unpublished) were synthesized in house and tested for their affinities in the Caco-2 cell assay.[59]

2.2.2. Conformational search in simulated water. The underlying concept for the calculation method for $\Delta G_{\mathrm{conf(ligand)}}$ proposed by Boström et al.[52] is that in order for a ligand to bind, it has to be transferred from an aqueous environment to a protein environment. To obtain the reference conformation compounds **16**–**35** were first submitted to a conformational search in simulated water. Several compounds displayed a preference for conformations with intramolecular H-bond interactions between the backbone and the ester/carbamate group of the side chain, corresponding to their global energy minimum conformation in water. However, whether this represents the correct situation in aqueous solution or is a result of a computational artifact is not clear since it is expected that surrounding water molecules and counterions will reduce the tendency for formation of intramolecular interactions of this kind. Such interactions may result in a distortion of the backbone, and these conformations were therefore not considered in this study. Instead the conformation lowest in energy without such interactions was regarded the global energy minimum in water.

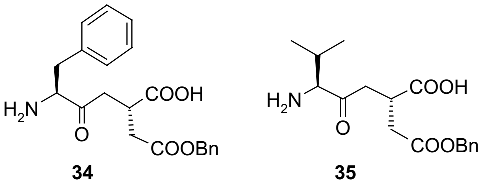

34
PheΨ[$COCH_2$]Asp(OBn)

35
ValΨ[$COCH_2$]Asp(OBn)

Figure 7. Structures of the ketomethylene-based prodrugs **34** and **35**.

A more complex situation was observed for Asp(OBn)-Sar (**23**) and Glu(OMe)-Sar (**24**), which had a preference for a *cis*-amide conformation in aqueous environment. It is known that the *cis*-conformation of Xaa-Sar derivatives is unusually stable in aqueous solution, illustrated by a *cis*-content of 39% reported for Gly-Sar.[31] This means that the calculated conformational properties observed for the backbones of Xaa(OR)-Sar (**23**–**24**) could not be considered as a computational artifact in the same way as for **13** and **14** in vacuo. However, in the intriguing study by Brandsch et al. of AlaΨ[CS–N]Pro, which is characterized by its slow *cis*/*trans*-isomerization rate, it was shown that an intracellular accumulation of the *trans*-conformation took place (92% intracellularly compared to 62% apically).[30] This was the first study unequivocally demonstrating that a *trans*-conformation was critical in order to retain hPEPT1 affinity and transport. Their subsequent study on natural Xaa-Pro dipeptides, also shown to have a considerable *cis*-conformational content, revealed a similar conformational dependent affinity pattern for this class of dipeptides.[31] This work also addressed the *cis*- and *trans*-conformations for Xaa-Sar dipeptides.[31] In conclusion, the molecules that bind to hPEPT1 (and subsequently are transported) originate from the conformational '*trans*-pool', which is in equilibrium with the '*cis*-pool'. Considering a rapid equilibrium, the main effect of this phenomenon is an underestimation of the affinity of the *trans*-conformation due to concentration effects. Consequently, the *trans*-conformations of **23** and **24** with lowest energy in simulated water were used as reference.

2.2.3. Constrained relaxation. In the study by Boström et al. the internal energy of the ligand in water was calculated by excluding the solvation energy term from the total energy in order to compare the energy values obtained in water and in vacuo (default $\varepsilon = 1$ in both cases).[52] In the present study a modification of this approach was used, where the backbone of the global energy minimum conformation obtained in water was energy minimized in vacuo with backbone constraints (using observed angles of ψ_1, ω_1, and $\varphi_2 \pm 0°$). This procedure is known as constrained relaxation, and an energy that could be directly compared with the energy of the bioactive conformation (calculated in vacuo, see below) was thereby obtained. To ensure that the deviations resulting from the constrained energy minimization procedure did not seriously affect the results, the resulting conformation in vacuo and the original global energy minimum conformation in water were superimposed and the root mean square (RMS) was calculated. The deviation (all atoms) was in all cases below 0.09 Å (results not shown), which implies a negligible influence.

2.2.4. Backbone alignment and $\Delta E_{\mathrm{bbone}}$ calculations. The backbone structures of the 20 model prodrugs **16**–**35** were subsequently aligned to the identified bioactive conformation by constrained energy minimization in vacuo. Finally, the energy difference between the aligned backbone conformation and the relaxed global energy minimum conformation in water, $\Delta E_{\mathrm{bbone}}$, was calculated (Tables 3 and 4). A negative $\Delta E_{\mathrm{bbone}}$ was obtained when the energy of the global minimum conformation was higher in water than in vacuo, and the energy of the bioactive conformation was between these two energy values.

2.2.5. Relationship between $\Delta E_{\mathrm{bbone}}$ and K_i values. The scatter plot for $\Delta E_{\mathrm{bbone}}$ versus log $1/K_i$ for compounds **16**–**35** revealed an inverse linear relationship (Fig. 8) with a conventional correlation coefficient (r^2) of 0.81. Due to the limited amount of affinity data available in the literature, the predictivity of the model was validated by internal prediction, giving a cross-validated correlation coefficient (q^2) for the whole data set of 0.80, demonstrating a highly predictive model. The r^2 value could be further divided into values of 0.87 and 0.78 for the compounds using R_1 attachment (**9**) and R_2 attachment (**11**), respectively (not statistically significant difference in slope for the two compound populations).

Qualitatively the plot revealed that a $\Delta E_{\mathrm{bbone}}$ value <1 kcal/mol is important to retain a high affinity ($K_i < 0.5$ mM) for hPEPT1, and that $\Delta E_{\mathrm{bbone}}$ values above this energy threshold result in medium to low affinity, according to the affinity classification scheme proposed by Brandsch et al.[8] A $\Delta E_{\mathrm{bbone}} > 3$ kcal/mol is likely to effectively abolish affinity for hPEPT1. This estimate is in accordance with the maximum conformational energy penalty of 2.5–3 kcal/mol for bioactive conformations suggested by Liljefors and Petterson.[57]

The chemical basis for the increased $\Delta E_{\mathrm{bbone}}$ of compounds with one D-configured stereocenter seems to be that alignment to the bioactive conformation results in an orientation of the incorrectly configured R-group that approaches an energetically disfavored eclipsed conformation relative to the amide bond (torsion angle 45–55°). Somewhat conflicting results have been obtained for the selectivity of compounds with one or more stereocenters with D-configuration,[29,60] but in general the affinities of dipeptides appear to be in the order L,L > D,L > L,D > D,D.[39] The stereoselectivity of hPEPT1 has generally been exclusively attributed to the 3D shape of the binding site, that is, the intermolecular interaction energy between ligand and protein. However, for a dipeptide this only holds true if it binds in a planar peptide backbone conformation, that is, the three backbone torsions having a strict *trans*- or *cis*-orientation (180° or 0°). Since the bioactive backbone conformation deviates from this picture, a contribution to the overall stereoselectivity of binding is expected also from $\Delta G_{\mathrm{conf(ligand)}}$. The affinities of the four isomers **21**–**22** and **32**–**33**, consisting of two enantiomeric pairs, were apparently contradictory as a D-configuration in R_2 resulted in a relative reduction in affinity for the Glu-Val derivatives **21**–**22**, whereas for the Val-Glu derivatives **32**–**33** it resulted in a relative increase in affinity. Introduction of valine results in an increased steric bulk close to the backbone compared to, for example, alanine. Therefore, irrespective of position a valine residue with incorrect stereochemistry (**21** and **33**) could be expected to have dramatic consequences on $\Delta E_{\mathrm{bbone}}$ and hence on affinity, as was also observed. Interestingly, $\Delta E_{\mathrm{bbone}}$ correctly predicted the K_i rank order not only of the individual enantiomeric pairs, but also of all four compounds ($r^2 = 0.995$). These results strongly suggest that it is not the position of the D-amino acid alone that determines the affinity of the pro-moiety, but also the nature of its R-group. Thus, the present study reveals that the energy required to adopt the bioactive conformation partly explains the experimentally observed stereochemical selectivity of hPEPT1, even if the method failed to predict the rank order for some of the diastereomers, that is, the D,L- and L,D-Ala-Xaa(Z) derivatives.

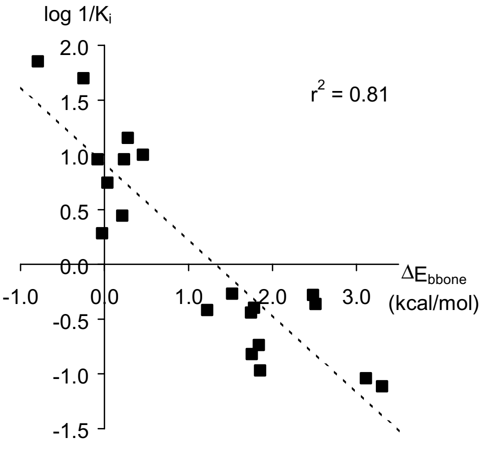

Figure 8. Relationship between $\Delta E_{\mathrm{bbone}}$ (kcal/mol) and log $1/K_i$ for compounds **16**–**35**. $\Delta E_{\mathrm{bbone}}$ is the calculated energy that is required in order to change the peptide backbone conformation from the global energy minimum conformation (in simulated water environment) to the identified bioactive conformation (in vacuo): $\psi_1 = 165°$, $\omega_1 = 180°$, and $\varphi_2 = 280°$.

It should also be mentioned that there are certain conceptual limitations to the approach presented in this study. Firstly, only the global energy minimum in water was used when calculating $\Delta E_{\mathrm{bbone}}$, that is, the conformational ensemble was not taken into consideration, an issue that also was addressed by Boström et al.[52] The fact that transfer of the ligand from an aqueous to a protein environment involves an energy dependent desolvation process is neither considered. Similarly, the energy barrier between the aqueous low energy conformation and the bioactive conformation, and also the possible conformational energy penalty resulting from χ-space (side chains) are ignored. Thus, it is somewhat surprising that the differences in $\Delta E_{\mathrm{bbone}}$ alone reflect the interaction with hPEPT1 to such an extent. However, it should be kept in mind that hPEPT1 is a promiscuous low-affinity transporter, and it can therefore be hypothesized that the binding site is a rather large water-filled pocket, where relatively unspecific intramolecular ligand–protein interactions take place once the ligand backbone has adopted the appropriate conformation.

In summary, the calculations showed a significant overall correlation between $\Delta E_{\mathrm{bbone}}$ and the K_i values, indicating that the present method will facilitate the design of novel pro-moieties. As only the pro-moieties with correct stereochemistry (ketomethylene and *N*-methylated derivatives) displayed a ΔE_{bbone} low enough to result in high affinity for hPEPT1, the immediate implications of the findings is to focus on the further development of prodrugs based on these kinds of pro-moieties. Considering the relatively simple computational procedures required, this approach can be used also by non-specialists in the field of computational chemistry. The results also encourage the development of a more detailed 3D pharmacophore for hPEPT1, into which ΔE_{bbone} should be incorporated as an important descriptor.

3. Conclusions

The bioactive conformation for hPEPT1 substrates in terms of binding was identified by ligand-based design, and was described by $\psi_1 \sim 165°$, $\omega_1 \sim 180°$, and $\varphi_2 \sim 280°$. A highly significant relationship between ΔE_{bbone} and K_{i} ($r^2 = 0.81$, $q^2 = 0.80$) was found for a series of model prodrugs with diverse pro-moieties, demonstrating the importance of considering the conformational energy penalty when predicting binding affinity. The results suggest a cutoff value for E_{bbone} of 1 kcal/mol in order to retain a high affinity for hPEPT1. It was also demonstrated that the choice of backbone structure and substitution pattern of the pro-moiety has major influence on the ability of the prodrug to adopt the bioactive conformation. Investigations of the conformational properties of dipeptidomimetic model prodrugs will therefore aid in the future design of optimized pro-moieties in a prodrug approach targeting hPEPT1.

4. Methods

4.1. Definitions

4.1.1. Backbone. The word 'backbone' in the context of energy minimization refers to all atoms of the peptide/peptidomimetic backbone from the *N*- to the *C*-terminus, including all atoms in the side chain not involved in model drug attachment (R_{bbone}: Gly, Ala, Val, Phe). Also the β-carbon (i.e., the atom closest to the backbone) of the side chain functioning as attachment point (R_{attach}: Asp, Glu, Orn, Lys) had to be included in order to define the stereochemistry. The atoms were defined using the Substructure submenu in Maestro.

4.1.2. Global energy minimum conformation in water. The conformation with lowest energy in simulated water without evident intramolecular electrostatic/H-bond interactions between the *N*- and *C*-termini or between the backbone and the side chain was defined as the global energy minimum conformation in water (see text for details).

4.2. Computational procedures

All molecular modeling studies were performed using the Maestro v3.0 interface to the MacroModel program v7.1[61] running on an SGI Octane workstation. The starting structures were all built with positively and negatively charged *N*- and *C*-termini, respectively. The MMFFs force field,[40] as implemented in MacroModel, with charges taken from the force field and a H-bond cutoff of 4 Å, was used for all energy calculations. The Truncated Newton Conjugate Gradient (TNCG) algorithm was used for all energy minimizations, with a maximum number of iterations of 500 and a convergence threshold of 0.012 kcal/mol Å (0.05 kJ/mol Å).

4.2.1. In vacuo. A distance dependent dielectric function ($\varepsilon = 4r_{ij}$) and a non-bonded cutoff of 7 Å for van der Waals interactions and 12 Å for electrostatics were used to mimic a protein environment.

4.2.2. Simulated water. The GB/SA continuum solvent model for H_2O developed by Still et al.[62] as implemented in MacroModel was used to simulate an aqueous environment, with a constant dielectric function ($\varepsilon = 1$). An extended non-bonded cutoff (van der Waals: 8 Å; electrostatics: 20 Å) was used.

4.2.3. Conformational search. A molecular mechanics based conformational analysis (Monte Carlo search algorithm) of 1000 steps was used for all compounds, except the β-lactam antibiotics (500 steps). The energy cutoff was generally set to $\Delta E = 3.6$ kcal/mol (15 kJ/mol) above the lowest energy conformation. Exceptions were made for Xaa(OR)Sar (**23** and **24**; $\Delta E = 8.4$ kcal/mol (35 kJ/mol)) to ensure that the *trans*-conformations with lowest energy were obtained.

4.2.4. 2D dihedral driving. 2D dihedral driving analysis in vacuo was performed by varying the torsion angles ψ_1 and φ_2 (for torsion angle definitions, see Fig. 2) independently from 0° to 360° in 10° increments, giving $36 \times 36 = 1296$ conformations for which the energy was calculated. In order to only obtain conformations with the appropriate *trans*-geometry for the ketomethylene isosteres (δ-ALA (**13**) and PheΨ[$COCH_2$]Gly (**14**)) and Gly-Sar (**15**), the ω_1 torsion was constrained to 180° ± 5° during the 2D search using a force constant (k) of 24 kcal/mol deg^2 (100 kJ/mol deg^2).

4.2.5. Constrained backbone relaxation of the global energy minimum conformation in water. To enable a direct comparison between the bioactive conformation (calculated in vacuo, see below) and the global energy minimum conformation in water, the backbone of the global energy minimum conformation in water was energy minimized in vacuo with torsional backbone constraints, using observed angles of ψ_1, ω_1, and $\varphi_2 \pm 0°$, $k = 240$ kcal/mol deg^2 (constrained relaxation). The energy of the resulting conformation was then recalculated without the constraints to get the actual energy. To ensure that the deviations resulting from this minimization procedure did not seriously affect the results, the global energy minimum conformation in water and its relaxed structure in vacuo were superimposed (all atoms) and the root mean square (RMS) deviations calculated.

4.2.6. Backbone alignment. In order to align the compound backbone with the bioactive conformation, the backbone was energy minimized in vacuo with torsional constraints corresponding to the obtained bioactive backbone conformation ($\psi_1 = 165°$, $\omega_1 = 180°$, and $\varphi_2 = 280°$, $k = 240$ kcal/mol deg^2). The energy of the resulting conformation was then recalculated without the constraints. For compounds with a non-symmetric R_{bbone} (Val, Phe) three different conformations could be obtained due to the rotational barriers of the χ torsion for R_{bbone} (Fig. 2B). The energies of these conformations were calculated by enforcing a rotation of χ in 60° increments for R_{bbone}, followed by constrained energy minimization as described above. The conformation with lowest energy was used in the subsequent calculations.

The energy change required for the backbone to adopt the bioactive conformation, ΔE_{bbone}, was calculated as the energy difference between the relaxed backbone and the aligned backbone conformation. The program package Simca-P 10.0 (Umetrics AB, Umeå, Sweden) was used for calculation of the q^2 value.

Acknowledgements

Financial support for this project was obtained from the Norwegian Research Council (128256/420), the Swedish Research Council (621-2001-1431), the Knut and Alice Wallenberg Foundation (98.176), and the Danish Medicinal Research Council via the Center for Drug Design and Transport and via project grant #22-01-0310. The initiative to this project was realized by a Marie Curie Fellowship of the European Community Program 'Improving the Human Research Potential and the Socio-Economic Knowledge Base' under contract number HPMT-CT-2001-00403. We thank Dr. Wolfgang Guba (F. Hoffmann-La Roche Ltd, Basel, Switzerland) for constructive initial discussions, and Frederick Leeson for valuable linguistic assistance.

References and notes

1. Fei, Y. J.; Kanai, Y.; Nussberger, S.; Ganapathy, V.; Leibach, F. H.; Romero, M. F.; Singh, S. K.; Boron, W. F.; Hediger, M. A. *Nature* **1994**, *368*, 563.
2. Liang, R.; Fei, Y. J.; Prasad, P. D.; Ramamoorthy, S.; Han, H.; Yang-Feng, T. L.; Hediger, M. A.; Ganapathy, V.; Leibach, F. H. *J. Biol. Chem.* **1995**, *270*, 6456.
3. Walter, E.; Kissel, T.; Amidon, G. L. *Adv. Drug Deliv. Rev.* **1996**, *20*, 33.
4. Yang, C. Y.; Dantzig, A. H.; Pidgeon, C. *Pharm. Res.* **1999**, *16*, 1331.
5. Brodin, B.; Nielsen, C. U.; Steffansen, B.; Frokjaer, S. *Pharmacol. Toxicol.* **2002**, *90*, 285.
6. Rubio-Aliaga, I.; Daniel, H. *Trends Pharmacol. Sci.* **2002**, *23*, 434.
7. Nielsen, C. U.; Brodin, B.; Jørgensen, F. S.; Frokjaer, S.; Steffansen, B. *Expert Opin. Ther. Pat.* **2002**, *12*, 1329.
8. Brandsch, M.; Knütter, I.; Leibach, F. H. *Eur. J. Pharm. Sci.* **2004**, *21*, 53.
9. Bretschneider, B.; Brandsch, M.; Neubert, R. *Pharm. Res.* **1999**, *16*, 55.
10. Moore, V. A.; Irwin, W. J.; Timmins, P.; Lambert, P. A.; Chong, S.; Dando, S. A.; Morrison, R. A. *Int. J. Pharm.* **2000**, *210*, 29.
11. Bai, J. P. F. *Pharm. Res.* **1995**, *12*, 1101.
12. Anand, B. S.; Patel, J.; Mitra, A. K. *J. Pharmacol. Exp. Ther.* **2003**, *304*, 781.
13. Beauchamp, L. M.; Orr, G. F.; de Miranda, P.; Burnette, T.; Krenitsky, T. A. *Antiviral Chem. Chemother.* **1992**, *3*, 157.
14. de Vrueh, R. L. A.; Smith, P. L.; Lee, C. P. *J. Pharmacol. Exp. Ther.* **1998**, *286*, 1166.
15. Covitz, K.-M. Y.; Amidon, G. L.; Sadée, W. *Biochemistry* **1998**, *37*, 15214.
16. Fei, Y. J.; Liu, W.; Prasad, P. D.; Kekuda, R.; Oblak, T. G.; Ganapathy, V.; Leibach, F. H. *Biochemistry* **1997**, *36*, 452.
17. Bolger, M. B.; Haworth, I. S.; Yeung, A. K.; Ann, D.; von Grafenstein, H.; Hamm-Alvarez, S.; Okamoto, C. T.; Kim, K. J.; Basu, S. K.; Wu, S.; Lee, V. H. L. *J. Pharm. Sci.* **1998**, *87*, 1286.
18. Yeung, A. K.; Basu, S. K.; Wu, S. K.; Chu, C.; Okamoto, C. T.; Hamm-Alvarez, S. F.; von Grafenstein, H.; Shen, W. C.; Kim, K. J.; Bolger, M. B.; Haworth, I. S.; Ann, D. K.; Lee, V. H. L. *Biochem. Biophys. Res. Commun.* **1998**, *250*, 103.
19. Kulkarni, A. A.; Haworth, I. S.; Lee, V. H. L. *Biochem. Biophys. Res. Commun.* **2003**, *306*, 177.
20. Kulkarni, A. A.; Haworth, I. S.; Uchiyama, T.; Lee, V. H. L. *J. Biol. Chem.* **2003**, *278*, 51833.
21. Meredith, D. *J. Biol. Chem.* **2004**, *279*, 15795.
22. The term model prodrug indicates that a relatively simple compound (e.g., an organic alcohol such as BnOH) is used as a model drug. The rational behind biological investigations of model prodrugs instead of 'real' prodrugs is their synthetic feasibility and ease of detection as a result of the incorporated UV-chromophore (e.g., BnOH derivatives). Additionally, interesting structural variations can readily be introduced in the attached 'drug', and such compounds are therefore valuable for investigating the properties of the binding pocket. Further, if the model prodrug shows poor affinity and/or transport properties, it is not reasonable to expect a successful outcome of a 'real' prodrug based on the same pro-moiety. This assumption is based on the inherent unfavorable properties of the drug compared to the model drug, that is, increased hydrophilicity and size.
23. Taub, M. E.; Moss, B. A.; Steffansen, B.; Frokjaer, S. *Int. J. Pharm.* **1998**, *174*, 223.
24. Ezra, A.; Hoffman, A.; Breuer, E.; Alferiev, I. S.; Mönkkönen, J.; El Hanany-Rozen, N.; Weiss, G.; Stepensky, D.; Gati, I.; Cohen, H.; Törmälehto, S.; Amidon, G. L.; Golomb, G. *J. Med. Chem.* **2000**, *43*, 3641.
25. Thomsen, A. E.; Friedrichsen, G. M.; Sørensen, A. H.; Andersen, R.; Nielsen, C. U.; Brodin, B.; Begtrup, M.; Frokjaer, S.; Steffansen, B. *J. Control. Release* **2003**, *86*, 279.
26. Våbenø, J.; Nielsen, C. U.; Ingebrigtsen, T.; Lejon, T.; Steffansen, B.; Luthman, K. *J. Med. Chem.* **2004**, *47*, 4755.
27. Knütter, I.; Hartrodt, B.; Theis, S.; Foltz, M.; Rastetter, M.; Daniel, H.; Neubert, K.; Brandsch, M. *Eur. J. Pharm. Sci.* **2004**, *21*, 61.
28. It should be noted that a high affinity does not necessarily mean that the compound is transported, but affinity is a prerequisite for transport.
29. Tamura, K.; Bhatnagar, P. K.; Takata, J. S.; Lee, C. P.; Smith, P. L.; Borchardt, R. T. *Pharm. Res.* **1996**, *13*, 1213.

30. Brandsch, M.; Thunecke, F.; Küllertz, G.; Schutkowski, M.; Fischer, G.; Neubert, K. *J. Biol. Chem.* **1998**, *273*, 3861.
31. Brandsch, M.; Knütter, I.; Thunecke, F.; Hartrodt, B.; Born, I.; Börner, V.; Hirche, F.; Fischer, G.; Neubert, K. *Eur. J. Biochem.* **1999**, *266*, 502.
32. Bailey, P. D.; Boyd, C. A. R.; Bronk, J. R.; Collier, I. D.; Meredith, D.; Morgan, K. M.; Temple, C. S. *Angew. Chem., Int. Ed. Engl.* **2000**, *39*, 506.
33. Daniel, H.; Morse, E. L.; Adibi, S. A. *J. Biol. Chem.* **1992**, *267*, 9565.
34. Daniel, H.; Morse, E.; Adibi, S. *J. Biol. Chem.* **1991**, *266*, 19917.
35. Moreover, the energy window for allowed conformations was set to 10 kcal/mol above the energy minimum, which seems excessive since the logarithmic relationship between the equilibrium constant K and the free energy of binding ($\Delta G = -RT\ln K$) states that every 1.4 kcal/mol contribution to ΔG gives a 10-fold reduction in binding affinity.
36. Gebauer, S.; Knütter, I.; Hartrodt, B.; Brandsch, M.; Neubert, K.; Thondorf, I. *J. Med. Chem.* **2003**, *46*, 5725.
37. Wenzel, U.; Thwaites, D. T.; Daniel, H. *Br. J. Pharmacol.* **1995**, *116*, 3021.
38. Tamura, K.; Lee, C. P.; Smith, P. L.; Borchardt, R. T. *Pharm. Res.* **1996**, *13*, 1663.
39. Brandsch, M.; Knütter, I.; Hartrodt, B.; Gebauer, S.; Theis, S.; Boll, M.; Rubio-Aliaga, I.; Born, I.; Thondorf, I.; Daniel, H.; Neubert, K. *Nova Acta Leopoldina* **2003**, *87*, 75.
40. Halgren, T. A. *J. Comput. Chem.* **1999**, *20*, 720.
41. Liljefors, T.; Gundertofte, K.; Norrby, P.-O.; Pettersson, I. In *Computational Medicinal Chemistry for Drug Discovery*; Bultinck, P., De Vinter, H., Langenaeker, W., Tollenaere, J. P., Eds.; Marcel Dekker: New York, 2004; pp 1–28.
42. Dantzig, A. H.; Bergin, L. *Biochim. Biophys. Acta* **1990**, *1027*, 211.
43. Dantzig, A. H.; Duckworth, D. C.; Tabas, L. B. *Biochim. Biophys. Acta* **1994**, *1191*, 7.
44. Li, J. B.; Hidalgo, I. J. *J. Drug Target.* **1996**, *4*, 9.
45. Swaan, P. W.; Tukker, J. J. *J. Pharm. Sci.* **1997**, *86*, 596.
46. Swaan, P. W.; Koops, B. C.; Moret, E. E.; Tukker, J. J. *Receptors Channels* **1998**, *6*, 189.
47. Döring, F.; Walter, J.; Will, J.; Föcking, M.; Boll, M.; Amasheh, S.; Clauss, W.; Daniel, H. *J. Clin. Invest.* **1998**, *101*, 2761.
48. Irie, M.; Terada, T.; Sawada, K.; Saito, H.; Inui, K.-I. *J. Pharmacol. Exp. Ther.* **2001**, *298*, 711.
49. Våbenø, J.; Lejon, T.; Nielsen, C. U.; Steffansen, B.; Chen, W.; Ouyang, H.; Borchardt, R. T.; Luthman, K. *J. Med. Chem.* **2004**, *47*, 1060.
50. Only one additional dipeptide ketomethylene isostere, the Arg-Phe derivative arphamenine A, has to date been investigated for hPEPT1 affinity and transport properties, and high affinity and hPEPT1 mediated transport was demonstrated also for this compound (Enjoh, M.; Hashimoto, K.; Arai, S.; Shimizu, M. *Biosci. Biotechnol. Biochem.* **1996**, *60*, 1893). Arphamenine B, the ketomethylene isostere of Arg-Tyr, has been shown to inhibit PEPT2 mediated uptake of dipeptides (Daniel, H.; Adibi, S. A. *FASEB J.* **1994**, *8*, 753), but translocation has not yet been investigated. However, due to the problems associated with the flexible and positively charged arginine side chain of the arphamenines in the 2D analysis, these compounds were not included in the present study.
51. Payne, J. W.; Payne, G. M.; Gupta, S.; Marshall, N. J.; Grail, B. M. *Biochim. Biophys. Acta* **2001**, *1514*, 65.
52. Boström, J.; Norrby, P. O.; Liljefors, T. *J. Comput. Aided Mol. Des.* **1998**, *12*, 383.
53. Meredith, D.; Temple, C. S.; Guha, N.; Sword, C. J.; Boyd, C. A. R.; Collier, I. D.; Morgan, K. M.; Bailey, P. D. *Eur. J. Biochem.* **2000**, *267*, 3723.
54. Addison, J. M.; Burston, D.; Dalrymple, J. A.; Matthews, D. M.; Payne, J. W.; Sleisenger, M. H.; Wilkinson, S. *Clin. Sci. Mol. Med.* **1975**, *49*, 313.
55. Marshall, G. R.; Motoc, I. In *Graphics and Drug Design*; Burgen, A. S. V., Roberts, G. C. K., Tute, M. S., Eds.; Elsevier: New York, 1986; pp 115–156.
56. Siebel, G. L.; Kollman, P. A. In *Comprehensive Medicinal Chemistry*; Hansch, C., Sammes, P. G., Taylor, J. B., Eds.; Pergamon: Oxford, 1990; pp 125–138.
57. Liljefors, T.; Pettersson, I. In *Textbook of Drug Design and Discovery*; Krogsgaard-Larsen, P., Liljefors, T., Madsen, U., Eds., 3rd ed.; Taylor & Francis: Amsterdam, 2002; pp 86–116.
58. Nicklaus, M. C.; Wang, S.; Driscoll, J. S.; Milne, G. W. *Bioorg. Med. Chem.* **1995**, *3*, 411.
59. Nielsen, C. U.; Elm, P.; Begtrup, M.; Steffansen, B., unpublished results.
60. Hidalgo, I. J.; Bhatnagar, P.; Lee, C. P.; Miller, J.; Cucullino, G.; Smith, P. L. *Pharm. Res.* **1995**, *12*, 317.
61. Mohamadi, F.; Richards, N. G. J.; Guida, W. C.; Liskamp, R.; Lipton, M.; Caufield, C.; Chang, G.; Hendrickson, T.; Still, W. C. *J. Comput. Chem.* **1990**, *11*, 440.
62. Still, W. C.; Tempczyk, A.; Hawley, R. C.; Hendrickson, T. *J. Am. Chem. Soc.* **1990**, *112*, 6127.
63. Terada, T.; Sawada, K.; Irie, M.; Saito, H.; Hashimoto, Y.; Inui, K.-I. *Pflug. Arch.* **2000**, *440*, 679.
64. Taub, M. E.; Moss, B. A.; Steffansen, B.; Frokjaer, S. *Int. J. Pharm.* **1997**, *156*, 219.